JACS
JOURNAL OF THE AMERICAN CHEMICAL SOCIETY

Article

pubs.acs.org/JACS

Chemical Synthesis, Doping, and Transformation of Magic-Sized Semiconductor Alloy Nanoclusters

Jiwoong Yang,[†,‡,#] Franziska Muckel,[§,#] Woonhyuk Baek,[†,‡] Rachel Fainblat,[†,‡,§] Hogeun Chang,[†,‡] Gerd Bacher,[*,§] and Taeghwan Hyeon[*,†,‡]

[†]Center for Nanoparticle Research, Institute for Basic Science (IBS), Seoul 08826, Republic of Korea

[‡]School of Chemical and Biological Engineering, and Institute of Chemical Processes, Seoul National University, Seoul 08826, Republic of Korea

[§]Werkstoffe der Elektrotechnik und CENIDE, University Duisburg-Essen, Bismarckstraße 81, 47057 Duisburg, Germany

DOI: 10.1021/jacs.7b02953
J. Am. Chem. Soc. 2017, 139, 6761−6770

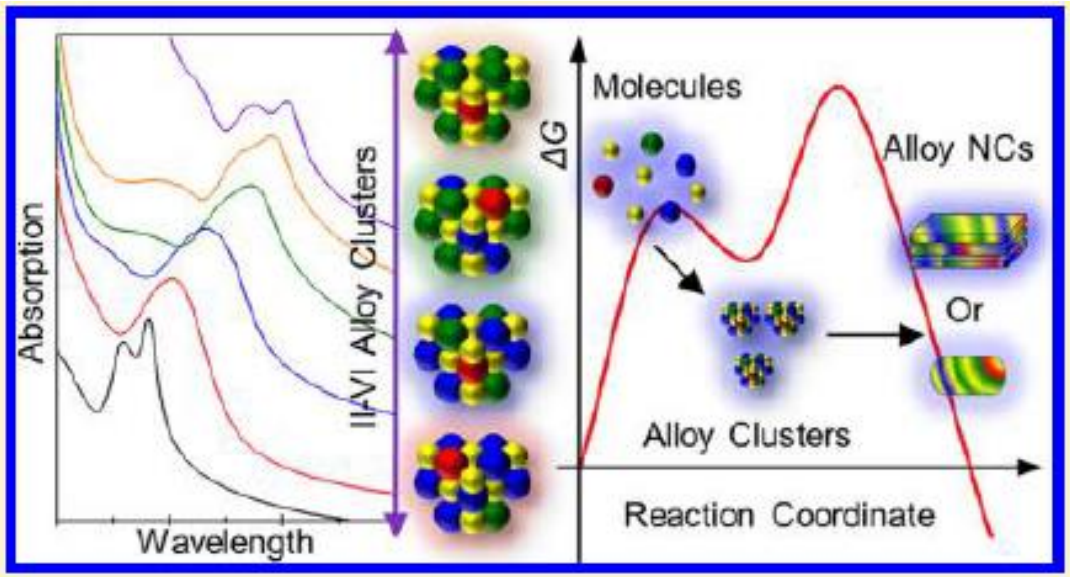

Manju C K
01.07.2017

Introduction

- In the last several decades, colloidal chemistry has provided effective ways to synthesize inorganic nanomaterials with unique properties originating from their sizes and shapes.

- Recently, research interests have been rapidly shifting from single-component to multicomponent nanostructures.

- Integration of multiple elements in nanoscale materials provides enhanced performance and/or multifunctionality for a wide range of applications such as energy, electronic, and biomedical applications.

- Various methods including doping, alloying, ion exchange, and heterodeposition have been employed to obtain multicomponent nanomaterials.

- In nanoscale metal-chalcogenide semiconductors, heteroatoms (e.g., cations) are usually incorporated by the adsorption on the surface of growing nanoparticles by forming bonds to counterions (e.g., chalcogen).

- Magic-sized nanoclusters, which consist of a discrete number of atoms, have been studied as important reaction intermediates between molecules and nanocrystals.

- In addition, alloying of II−VI semiconductor nanocrystals is usually achieved at high temperature above 250 °C, where clusters cannot be stabilized.

In this paper

- Chemical synthesis, doping, and transformation of magic-sized alloy clusters based on II−VI semiconductors is presented.

- Successfully obtained ternary and quaternary alloy clusters using room-temperature Lewis acid− base reactions.

RESULTS AND DISCUSSION

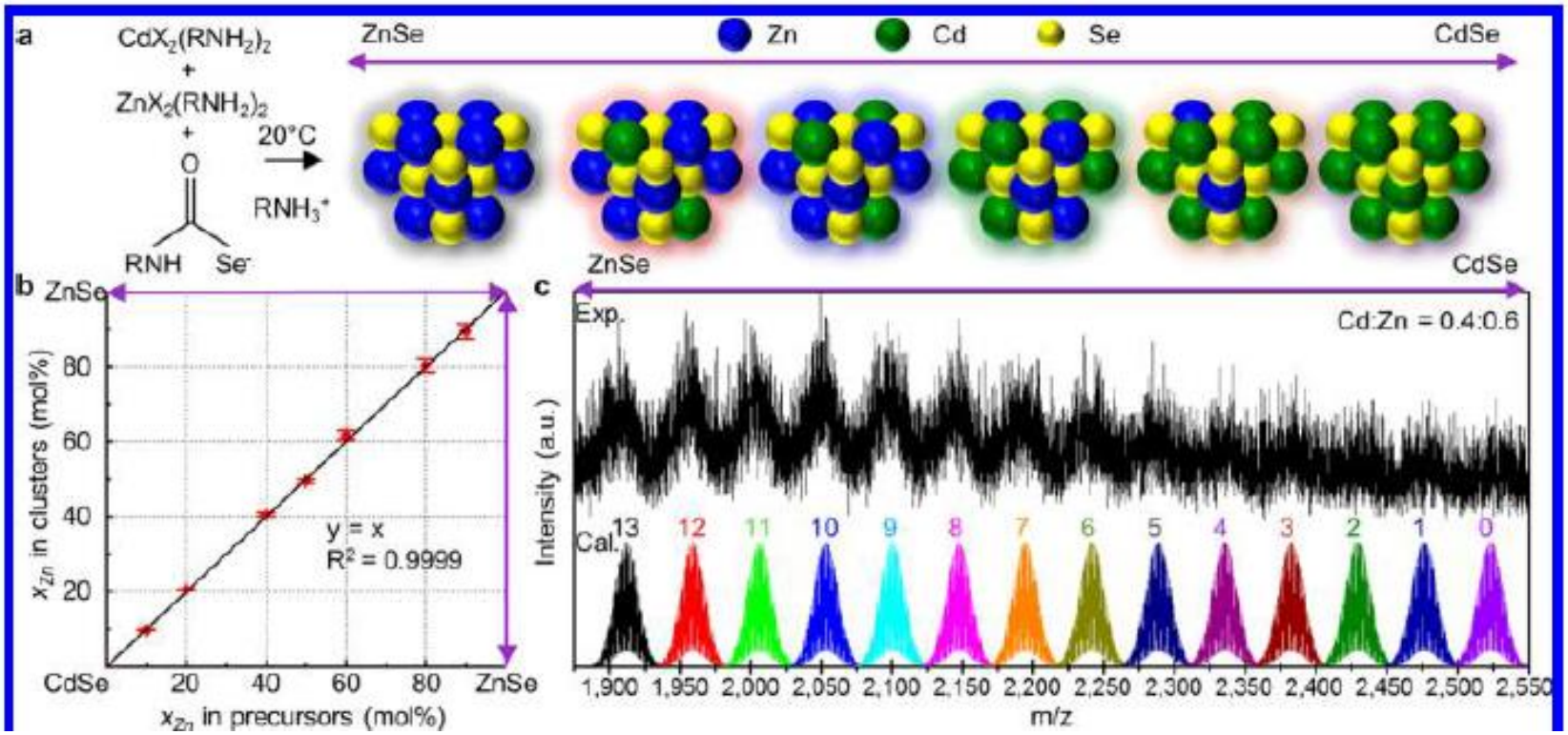

(a) A schematic illustration of the synthesis of the alloy II−VI semiconductor clusters. (b) The average cation molar ratio of the alloy clusters with respect to the molar ratio of the starting reagents. (c) Mass spectrum of the alloy clusters with an average composition of $Zn_{0.6}Cd_{0.4}Se$. The simulated spectra of $Zn_xCd_{13-x}Se_{13}$ (x = 0−13) are shown below the experimental data for comparison.

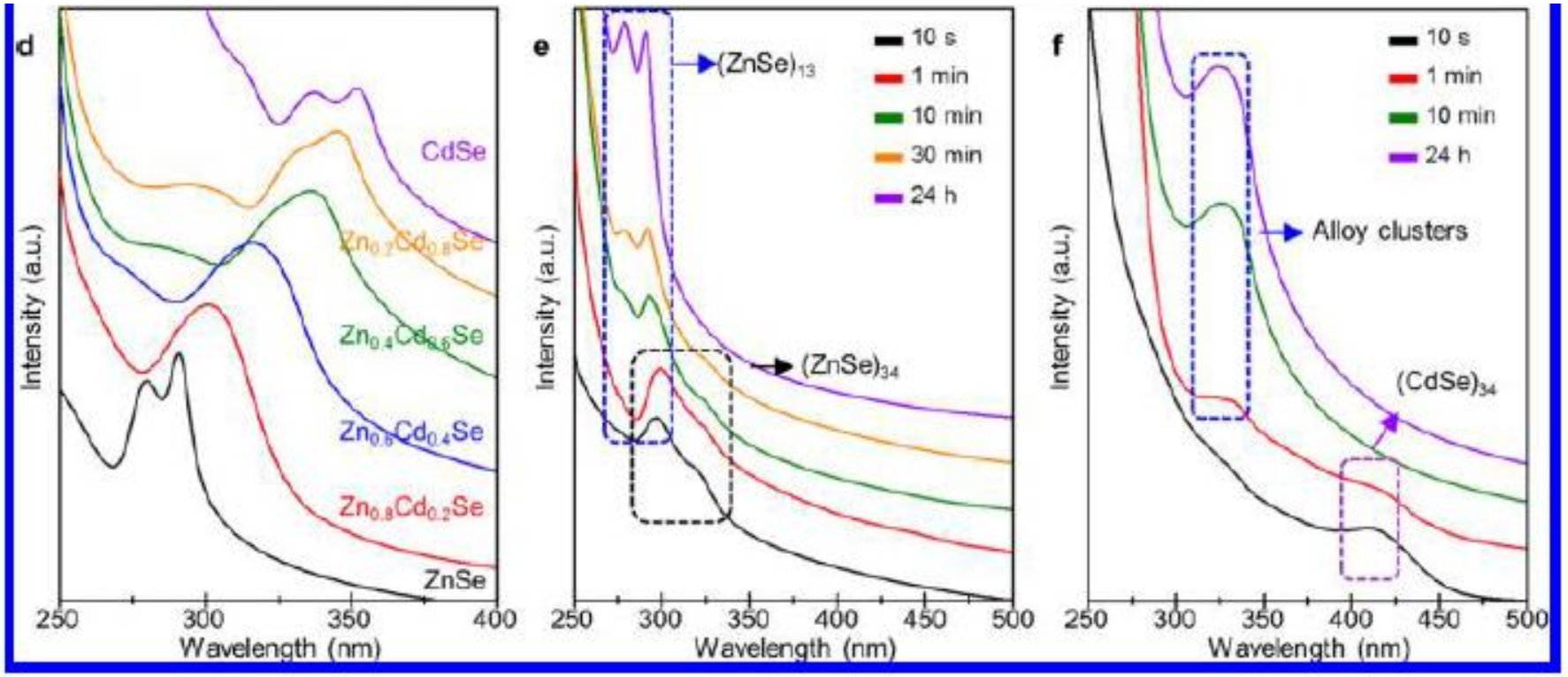

(d) Absorption spectra of the as-synthesized alloy clusters with various compositions. (e) Absorption spectra from the reaction mixture during the synthesis of the ZnSe clusters. $(ZnSe)_{34}$ clusters are observed before the formation of the $(ZnSe)_{13}$ clusters. (f) Absorption spectra from the reaction mixture during the synthesis of alloy clusters. $(CdSe)_{34}$ clusters are observed before the formation of the $Zn_xCd_{13-x}Se_{13}$ (x = 0−13) clusters.

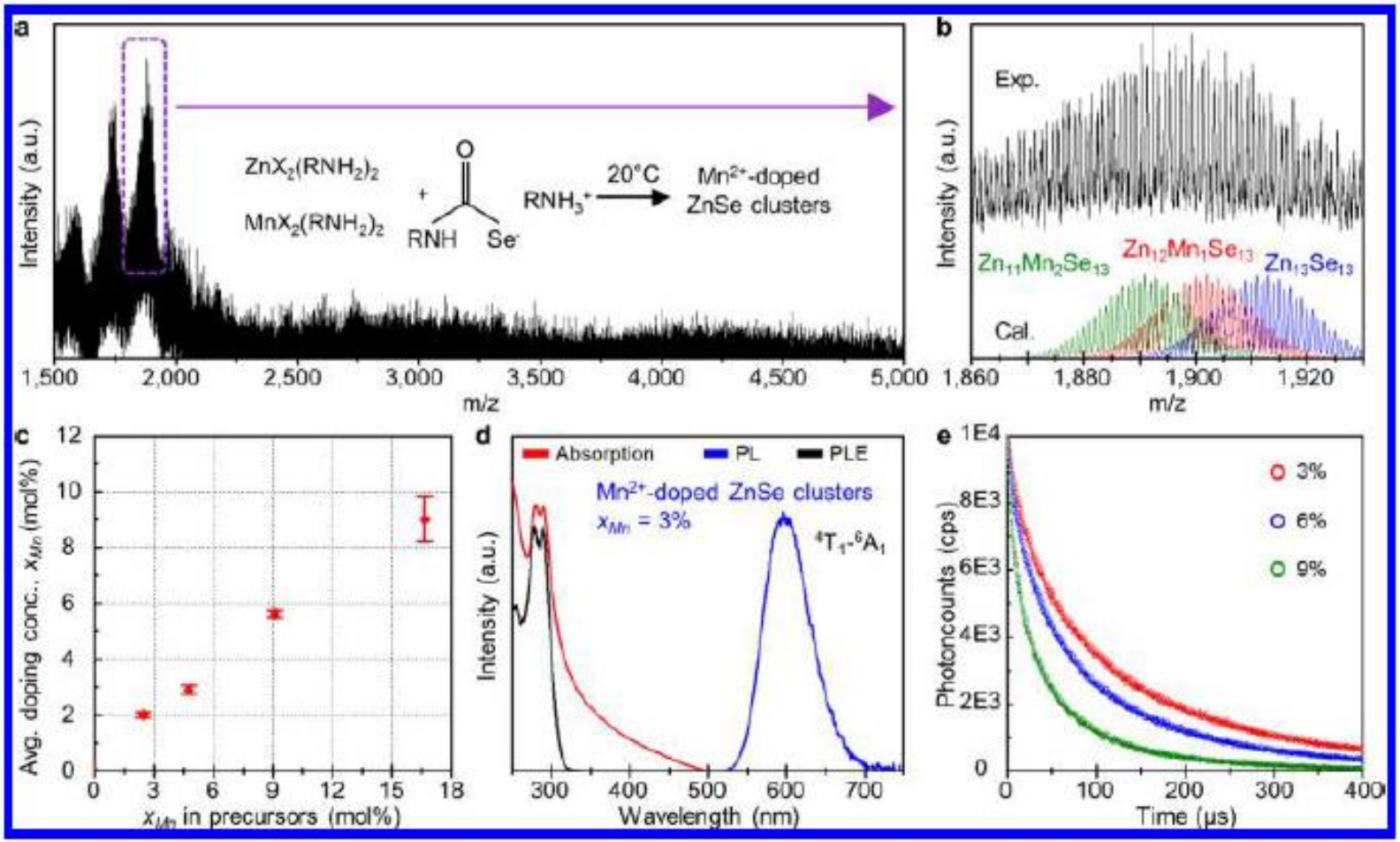

(a) Mass spectrum of Mn^{2+}-doped ZnSe clusters (xMn = 6%). (b) High resolution mass spectrum (reflectance mode) of the main peaks within the dashed box in panel (a). The simulated isotopic distributions of $Zn_{13}Se_{13}$ (blue), $Zn_{12}Mn_1Se_{13}$ (red), and $Zn_{11}Mn_2Se_{13}$ (green) are displayed below the experimental data (black) for comparison. (c) The final average doping concentration of the ZnSe clusters with respect to the initial ratio of Mn in precursors. (d) Absorption (red), PL (blue), and PLE (black) spectra of Mn^{2+}-doped ZnSe clusters (xMn = 6%). (e) Time-resolved PL spectra of Mn^{2+}-doped ZnSe clusters with different doping concentrations.

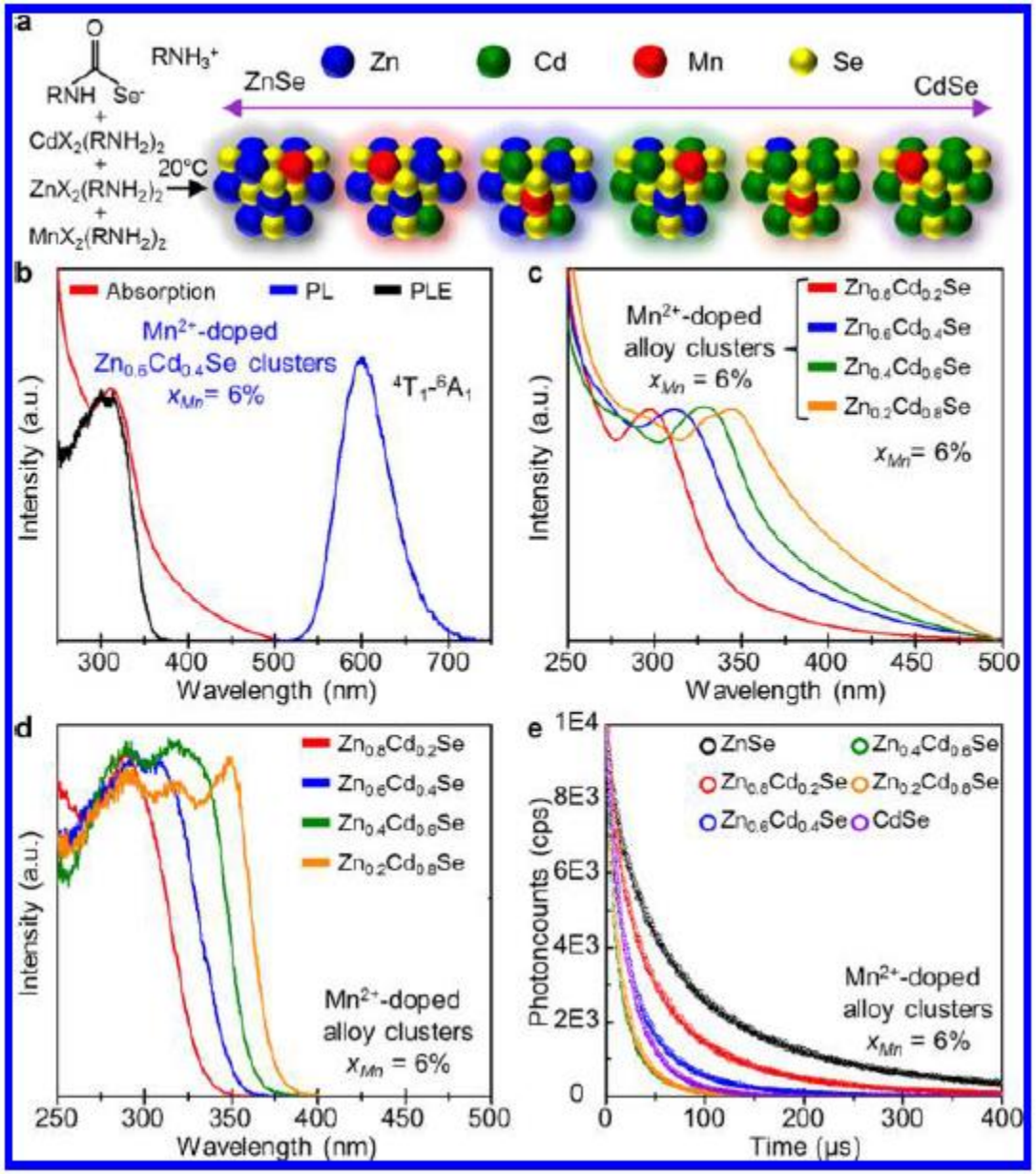

(a) A schematic showing the synthesis of the Mn^{2+}-doped II–VI semiconductor alloy clusters. (b), Absorption (red), PL (blue), and PLE (black) spectra of Mn^{2+}-doped $Zn_{0.6}Cd_{0.4}Se$ clusters (xMn = 6%). (c) Absorption, (d) PLE, and (e) time-resolved PL spectra of the Mn^{2+}-doped alloy clusters with various compositions (xMn = 6%).

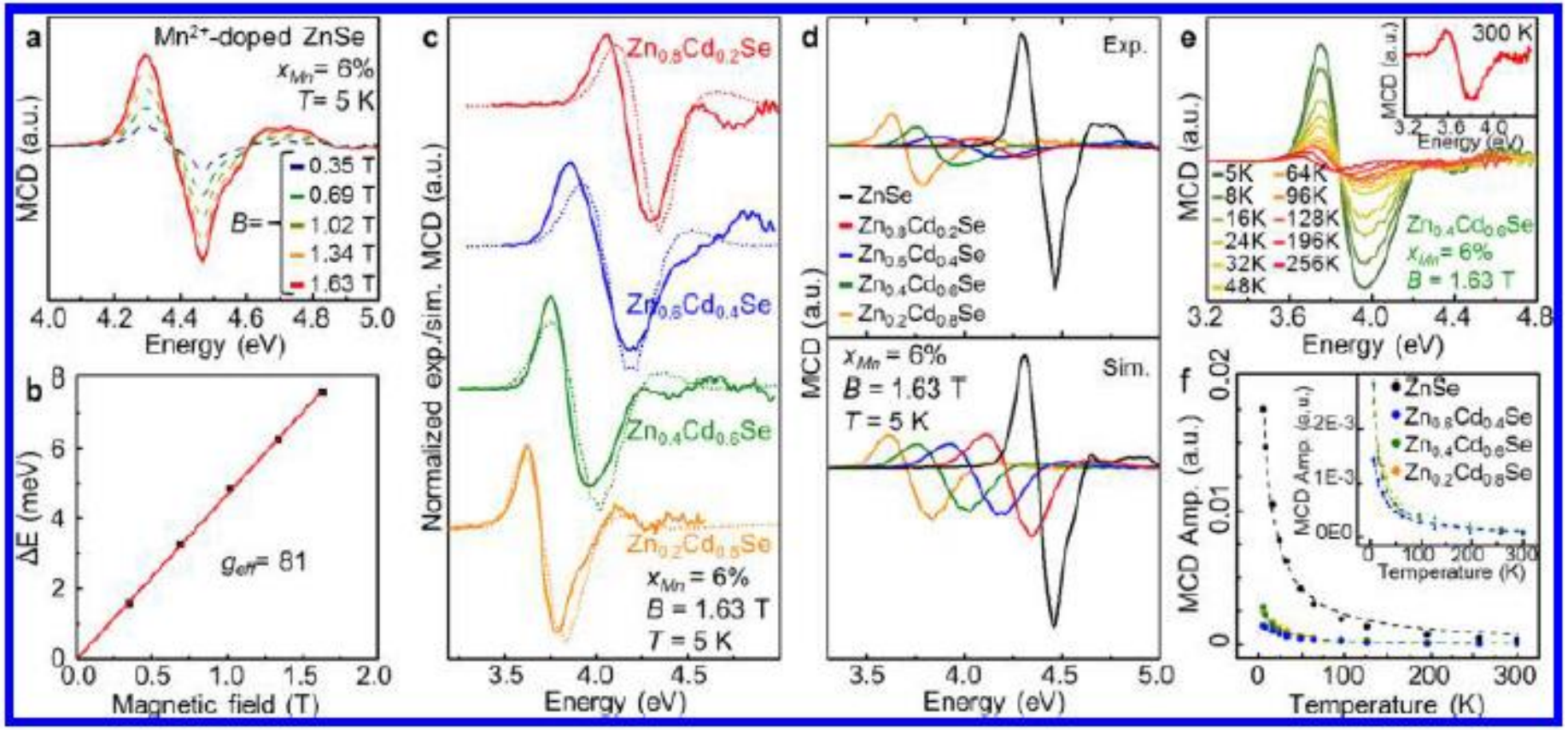

Magneto-optical properties of the Mn^{2+}-doped alloy clusters. (a) MCD spectra of the Mn^{2+}-doped ZnSe clusters (xMn = 6%) at 5 K. (b) Giant Zeeman splittings extracted from panel (a). (c) Normalized experimental (solid lines) and simulated (dashed lines) MCD spectra of the alloyed clusters (xMn = 6%) with various compositions. (d) Comparison of the experimental and simulated MCD spectra showing the MCD amplitudes. (e) Temperature-dependent MCD spectra of Mn2+-doped $Zn_{0.4}Cd_{0.6}Se$ clusters at 1.63 T. A room-temperature spectrum (300 K, red line) is shown in the inset. (f) Temperature-dependent behavior of the MCD amplitude of the alloy clusters with different compositions at 1.63 T.Brillouin fits (dashed line) are also displayed. The inset shows the magnified data on a different y scale.

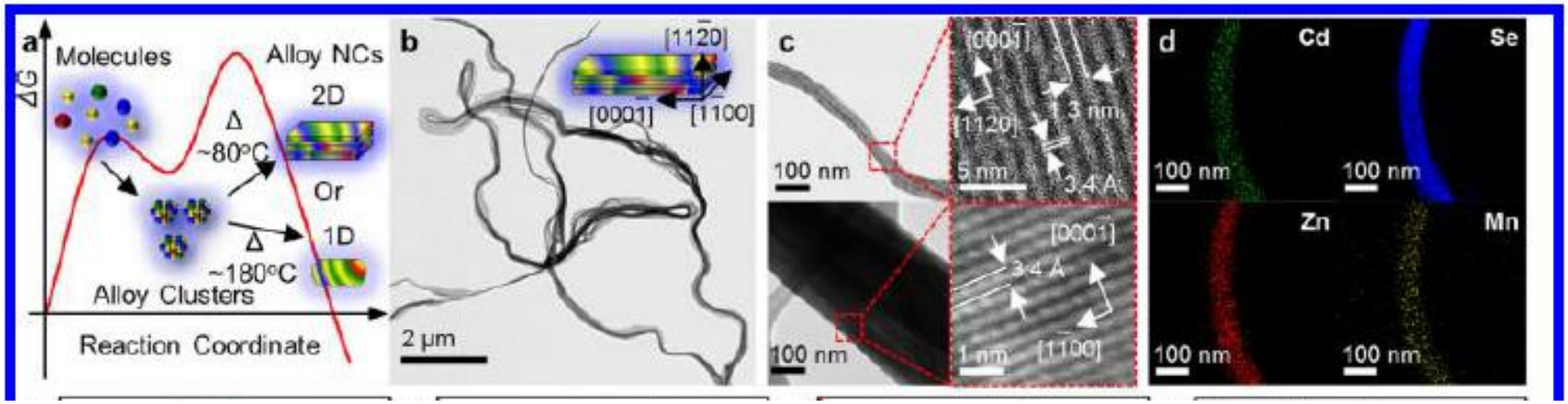

(a) Schematic illustration showing formation mechanism of alloy nanocrystals from alloy clusters. (b) Low resolution TEM and (c) HRTEM images of Mn^{2+}-doped $Cd_{0.8}Zn_{0.2}Se$ quantum nanoribbons (xMn =6%). HRTEM image of the edges (top) and top view (bottom) of the lamellar structured nanoribbons. The illustration in panel (b) shows the crystallographic nature of the nanoribbons. (d) EDS images of the alloy nanoribbons for Cd, Se, Zn, and Mn.

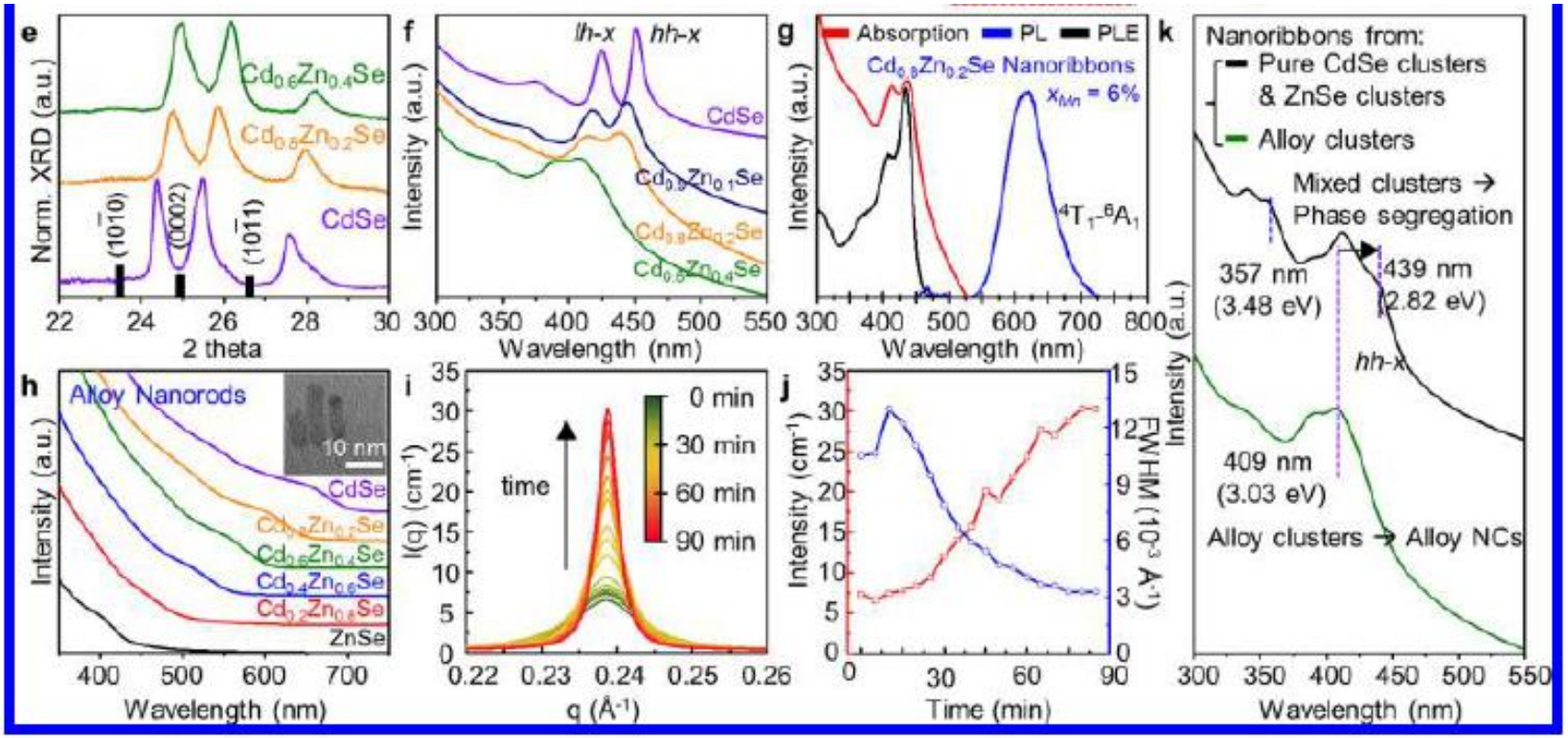

(e) Synchrotron HRPD patterns of the alloy nanoribbons. The diffraction peaks (black bars) for bulk wurtzite-CdSe (JCPDS# 65−3415) are shown. (f) Absorption spectra of the alloy quantum nanoribbons. (g) Absorption (red), PL (blue), and PLE (black) spectra of the Mn^{2+}-doped $Cd_{0.8}Zn_{0.2}Se$ quantum nanoribbons. (h) Absorption spectra of alloy nanorods obtained from the alloy clusters. The inset shows the TEM image of $Cd_{0.8}Zn_{0.2}Se$ nanorods. (i) In situ SAXS data and (j) their intensity and line width as a function of time during alloy nanoribbon synthesis from the alloy clusters. (k) Comparison of the absorption spectra of nanoribbons synthesized starting from $Cd_{0.6}Zn_{0.4}Se$ alloy clusters (green) and a mixture of CdSe clusters and ZnSe clusters (black; CdSe:ZnSe = 0.6:0.4).

Conclusion

- Synthesis, doping, and transformation of multielement magic-sized alloy clusters using Lewis acid−base reactions at room-temperature is demonstrated.

- This method can easily produce alloy clusters ($Zn_xCd_{13-x}Se_{13}$ (x = 0−13)), and their composition can be readily tuned between pure CdSe and pure ZnSe, allowing a wide variation of the bandgap in the high-energy range.

- Transition metal doping of these alloy clusters produces diluted magnetic alloy semiconductors whose bandgap is controllable up to the highest energy regime reported so far.